RCS characterization of sea clutter by using the α-stable distributions

Anthony Fiche*, Ali Khenchaf*, Jean-Christophe Cexus*, Majid Rochdi* and Arnaud Martin†

* LabSticc, UMR CNRS 6285, ENSTA-Bretagne, Brest, France, {fichean,khenchal,cexusje,rochdima}@ensta-bretagne.fr
† Université de Rennes 1, IRISA, Lannion, France, arnaud.martin@univ-rennes1.fr

Keywords: Sea surfaceRCS, bistatic scattering, α-stable distributions.

Abstract

In this paper, we propose a comparative statistical study of the ocean bistatic scattering which is useful in a problem of maritime radar target detection. We firstly introduce the electromagnetic properties and geometrical aspects of the sea surface. The scattered field of the sea surface is computed from the Physical Optics (PO) and compared with the Kirchhoff Approximation (KA) and the Small Perturbations Method (SPM). Early works have already characterized the Radar Cross Section (RCS) with a statistical model as the Weibull and $\mathcal{K}$ distributions. However, these models are limited especially when the probability density function of the sea surface RCS has a heavy tail. Consequently, we use a family of laws called the α-stable distributions. We compare the results obtained with each model by using a Kolmogorov-Smirnov test from several random sea surfaces and give a confidence interval for the estimated parameters of the α-stable distribution. We finally analyse the impact of distribution errors on detection performance.

1 Introduction

The characterization of sea clutter is a fundamental step for a radar system conception, especially to detect a target within sea clutter. For example, the scattered field from complex objets on sea surface has been computed [4]. The sea clutter is estimated from two methods :
– a statistical modeling from observations.
– a physical modeling from environmental phenomena.
The statistical modeling is often used thanks to its simplicity of implementation. The physical modeling is developed in parallel and is compared to the statistical modeling. In this paper, a statistical modeling is used to characterize the probability density function of the sea surface RCS.
In the literature, some statistical laws have been used to characterized the sea clutter from its probability density function. In practice, the sea clutter is non-gaussian and spiky. Various distributions have been used to fit the sea clutter such as the Weibull distribution [9, 14] or the $\mathcal{K}$ distribution [17, 16]. The phenomena of heavy-tails and asymmetry can be observed on the probability density function of the sea surface RCS. In probability theory, heavy-tailed distributions are probability distributions whose tails are not exponentially bounded : they have heavier tails than the exponential distribution. A skewed (non-symmetric) distribution is a distribution in which there is no mirror-imaging. A class of distributions exhibits these constraints : the α-stable distributions.
In the context of sea clutter modeling, the α-stable distributions have been exclusively used in the imagery domain. For example, the clutter has been modeled in ultra-wideband (UWB) Synthetic Aperture Radar (SAR) images [3]. The α-stable distributions characterize the speckle within SAR images [2]. In [13], the α-stable distributions are used to fit the RCS of sea surface and ship. However, this approach is limited because the RCS is computed in a backscattering configuration.
The remainder of this paper is organized in the following manner. In section 2, we characterize the sea surface model and develop the computation of the scattered field by a sea surface. In section 3, we enumerate the continuous probability density functions used to estimate the sea surface RCS : Weibull, $\mathcal{K}$ and α-stable distribuions. In section 4, we simulate the RCS depending on angle for several sea surface in a bistatic configuration and compare the quality of modelss with a Kolmogorov-Smirnov test. We finally give a confidence interval for the parameters of the α-stable distributions and analyse the impact of distribution errors on detection performance.

2 Sea surface RCS

In this section, the electromagnetic characteristics and geometrical aspects of sea surface are detailed. The scattered field will be computed from a deterministic sea surface by using the Physical Optics.

2.1 Sea surface modeling

The scattered field of the sea surface depends both on its electromagnetic characteristics and its geometrical aspects. The electromagnetic characteristics of the sea are defined by the dielectric constant which depends on the temperature and the salinity [11]. The geometric properties of the sea surface can be modeled as a random height as a function of the position (x, y) and time t. However, the power spectral density of the wave height is generally given to model the waves. In this contribution, the waves are generated by using the Elfouhaily [8] sea spectrum. Indeed, the Elfouhaily sea spectrum gives a comprehensive directional wave spectrum valid for the full range of gravity and capillary waves. This model is also agreed with the slope model proposed by Cox and Munk [5, 6]. Two sea surfaces have been generated with the Elfouhaily sea spectrum, with a wind

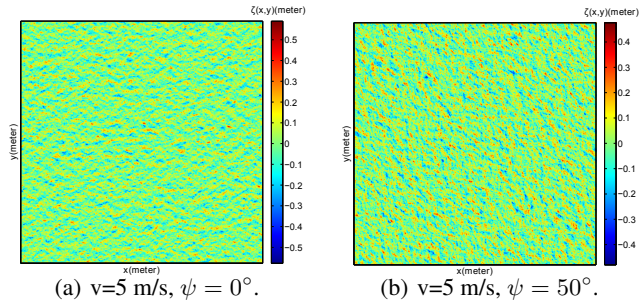

(a) v=5 m/s, $\psi = 0°$. (b) v=5 m/s, $\psi = 50°$.

FIGURE 1 – Example of surface generated with the Elfouhaily sea spectrum.

speed v=5 m/s and wind direction $\psi = 0°$ (Figure 1(a)) and $\psi = 50°$ (Figure 1(b)). The wind direction has a non negligible impact on the waves orientation.
To sum up, the sea surface are generated by using the Elfouhaily sea spectrum. The computation of scattered field by the sea surface is developed in the below section.

2.2 Scattering model

The scattered field is estimated by using the Physical Optics (PO). The initial point of PO is the currents produced by an incoming electromagnetic wave $(\mathbf{E}_i, \mathbf{H}_i)$. The electromagnetic wave creates the induced magnetic $\mathbf{J}_m$ and electric $\mathbf{J}_e$ currents given by :

$$\mathbf{J}_m = -\mathbf{n} \times \mathbf{E} \quad \mathbf{J}_e = \mathbf{n} \times \mathbf{H} \tag{1}$$

where n is the unit normal vector to the surface, $\mathbf{E}$ and $\mathbf{H}$ are respectively the total electric and magnetic fields at the surface.
The incident field can be considered as a plane wave if the source illuminating the target is at a far enough distance. The scattering field from the illuminated surface S is given by :

$$\mathbf{E}_s = \frac{\mathbf{i}ke^{(-\mathbf{i}\mathbf{k}R)}}{4\pi R} \int_S [\mathbf{k}_s \times (\eta \mathbf{k}_s \times \mathbf{J}_e + \mathbf{J}_m)] e^{-\mathbf{i}k\mathbf{k}_s.\mathbf{r}} ds \tag{2}$$

where k is the wavenumber, R is the distance between the center of the referential and the receiver, $\mathbf{k}_i$ and $\mathbf{k}_s$ are respectively the unit directional vectors of the incident and scattering electromagnetic wave. The parameter η is the impedance of the medium and $\mathbf{r}$ is the position vector of a point in S. The equation (2) can be solved by decomposing the sea surface into triangular subregions [7].

3 Models of estimation

Several models have been used for non-Gaussian amplitude sea clutter returns :
– the Weibull distribution.
– the $\mathcal{K}$ distribution.
– the α-stable distribution.
Amongst the more well known model is the Weibull distribution. The $\mathcal{K}$ distribution provides a good fit to sea clutter amplitude returns. Recently, the α-stable distribution has been used to model sea clutter. The probability density functions and the cumulative density functions are developed in the below section and used in the section 4.

3.1 The Weibull distribution

A random variable X is said to be a Weibull distribution [18] with parameters $\lambda \in \mathbb{R}^{+*}$ and $k \in \mathbb{R}^{+*}$, noted $X \sim \mathcal{W}(\lambda, k)$, if its probability density function has the form :

$$f_{\mathcal{W}(\lambda,k)}(x) = \begin{cases} \frac{k}{\lambda}\left(\frac{x}{\lambda}\right)^{(k-1)} e^{-\left(\frac{x}{\lambda}\right)^k} & \text{if } x \geq 0 \\ 0 & \text{otherwise.} \end{cases} \tag{3}$$

where λ is the scale parameter and k is the shape parameter. The cumulative density function associated to a random variable $X \sim \mathcal{W}(\lambda, k)$ is :

$$F_{\mathcal{W}(\lambda,k)}(x) = \begin{cases} 1 - e^{-\left(\frac{x}{\lambda}\right)^k} & \text{if } x \geq 0 \\ 0 & \text{otherwise.} \end{cases} \tag{4}$$

3.2 The $\mathcal{K}$ distribution

The $\mathcal{K}$ distribution has been first introduced by Jakeman and Pusey [10] to model the sea clutter. A random variable X is said to be a $\mathcal{K}$ distribution with parameters $\nu > 1$ and $a \in \mathbb{R}^{+*}$, noted $X \sim \mathcal{K}(\nu, a)$, if its probability density function has the form :

$$f_{\mathcal{K}(a,\nu)}(x) = \begin{cases} \frac{2}{a\Gamma(\nu+1)}\left(\frac{x}{2a}\right)^{\nu+1} K_\nu\left(\frac{x}{a}\right) & \text{if } x \geq 0 \\ 0 & \text{otherwise.} \end{cases} \tag{5}$$

where a is the scaling parameter, ν is the shape parameter, $\Gamma(.)$ the gamma function and K_ν is the modified Bessel function of the second kind of order ν [1].
The cumulative density function [1] associated to a random variable $X \sim \mathcal{K}(\nu, a)$ is :

$$F_{\mathcal{K}(a,\nu)}(x) = \begin{cases} 1 - \frac{1}{\Gamma(\nu+1)2^\nu}\left(\frac{x}{a}\right)^{\nu+1} K_{\nu+1}\left(\frac{x}{a}\right) & \text{if } x \geq 0 \\ 0 & \text{otherwise.} \end{cases} \tag{6}$$

3.3 The α-stable distribution

The French mathematician Paul Lévy introduced a family of distributions called the α-stable distributions [12].
A random variable X is said α-stable, noted $X \sim S_\alpha(\beta, \gamma, \delta)$, if its characteristic function is [19] :

$$\phi_{S_\alpha(\beta,\gamma,\delta)}(t) = \begin{cases} e^{(it\delta - |\gamma t|^\alpha [1 + i\beta \tan(\frac{\pi\alpha}{2}) s(t)(|t|^{1-\alpha} - 1)])} & \text{if } \alpha \neq 1 \\ e^{(it\delta - |\gamma t|[1 + i\beta \frac{2}{\pi} s(t) \log|t|])} & \text{if } \alpha = 1 \end{cases} \tag{7}$$

with $\alpha \in]0, 2]$ the characteristic exponent, $\beta \in [-1, 1]$ the skewness parameter, $\gamma \in \mathbb{R}^{+*}$ the scale parameter, $\delta \in \mathbb{R}$ is the location parameter and $s(t)$ the sign function.

1. Refers to [1] for the properties of the Bessel function to compute the cumulative density function

The representation of an α-stable probability density function, noted $f_{S_\alpha(\beta,\gamma,\delta)}$, is obtained by calculating the Fourier transform of its characteristic function :

$$f_{S_\alpha(\beta,\gamma,\delta)}(x) = \int_{-\infty}^{\infty} \phi_{S_\alpha(\beta,\gamma,\delta)}(t) e^{(-itx)} dt \qquad (8)$$

The cumulative density function of an α-stable distribution is computed numerically.
In the remainder of this paper, the probability density function of the sea surface RCS (Weibull, $\mathcal{K}$ and α-stable) is estimated by using the Least Squares Estimation (LSE) because the LSE minimizes the least-squares error.

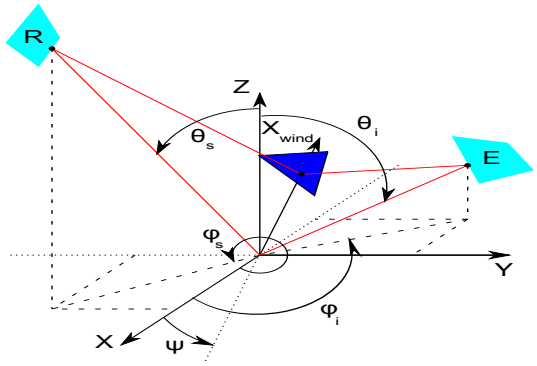

FIGURE 2 – Geometrical configuration.

4 Experiments results

The electromagnetic characteristics and the geometrical aspects of the sea surface have been developed in section 2 and the scattered field is estimated by using the Physical Optics. Notice that the angles used in the following are defined according to Figure 2. A dataset has been created with 500 deterministic sea surfaces (30×30) m-sized for the below configuration : wind speed $v = 5$ m/s, wind direction $\psi = 0°$, salinity $S = 35$ ppt, temperature $T = 20°C$, θ_i and $\theta_s \in [0°; 90°]$. The operating frequency is 10 GHz. The scattering coefficients σ_{mn} is dependent on wave polarizations in emission m and in reception n (in the following V means vertical and H means horizontal).
For the statistical study, θ_s is considered as a random variable for a fixed emitter $\theta_i = 30°$. The PO result (average of 10 RCS in this example) seems to indicate good

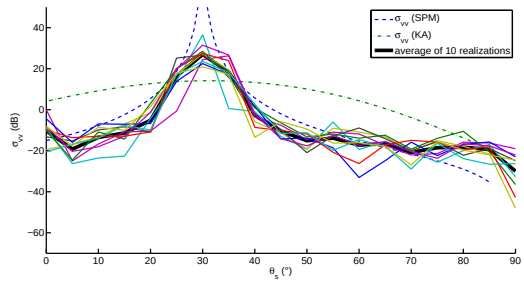

FIGURE 3 – Bistatic RCS of a random sea surface generated 10 times for a vv-polarization with $\theta_i = 30°$.

accuracy with results obtained by the Small Perturbations Method [15] (SPM) (we represent also the Kirchhoff Approximation result [15] (KA)) (see Figure 3). The parameter $\theta_s = 45°$ is then fixed to build a histogram of RCS from 50 deterministic sea surface (Figure 4). The histogram is estimated by the models described in section 3. The same step is realized 15 times. The same study is realized by fixing $\theta_i \in [0°; 90°]$ and by considering θ_s as a random variable. Note that we observe a reverse skew to the data. This phenomenon depends on the generation of deterministic sea surface. Indeed, the scattered field from a triangular subregion computed from the Physical Optics is null if the surface is not illuminated.

4.1 Goodness-of-fit test

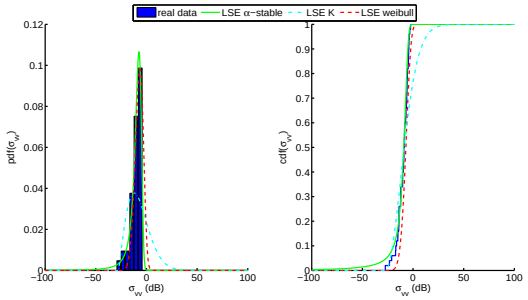

FIGURE 4 – An example of RCS and its estimations with $\theta_i = 45°$ and $\theta_s = 30°$.

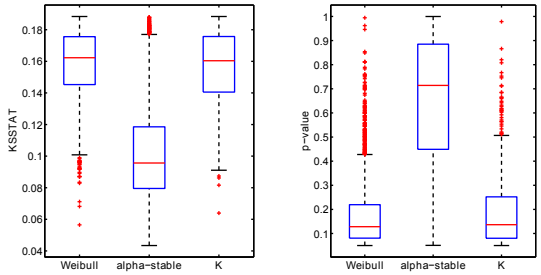

FIGURE 5 – Boxplots for the KSSTAT and the p-value.

The quality of a model can be evaluate by using a test of goodness-of-fit such as the χ^2 test and the Kolmogorov-Smirnov test (K-S test). The χ^2 goodness-of-fit depends on an adequate sample size for the approximations to be valide. In the remainder of this paper, the K-S test is used because this test is based from the cumulative density function and it will be more convenient to compute. We test the null hypothesis H_0 "the samples X with some unknown distribution $\mathbb{L}$ is equal to a particular distribution $\mathbb{L}_0$" :

$$H_0 : \mathbb{L} = \mathbb{L}_0, H_1 : \mathbb{L} \neq \mathbb{L}_0 \qquad (9)$$

The Kolmogorov-Smirnov test at the 5 % significance level compares the data cumulative distribution function with the cumulative density function of the fitted distribution. The distribution models are compared by boxplot, by precising

the p-value (the critical value to reject the null hypothesis) and the ksstat (the greatest discrepancy between the observed and expected cumulative frequencies). The percentage

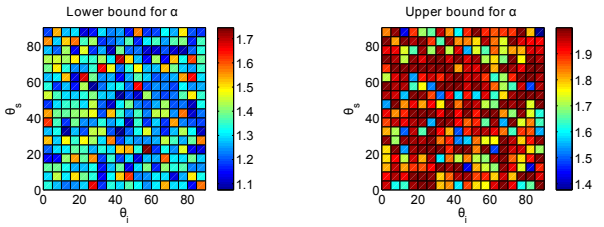

(a) Parameter α.

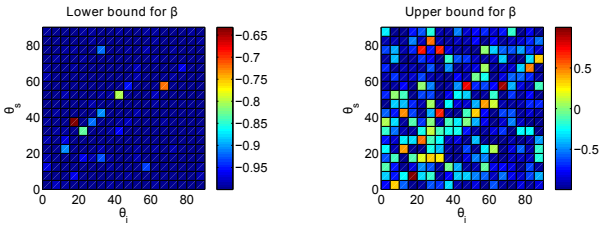

(b) Parameter β.

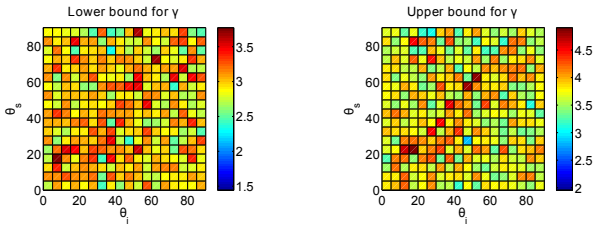

(c) Parameter γ.

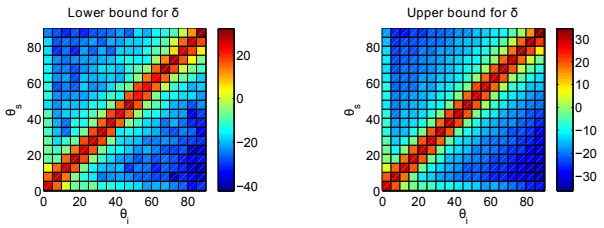

(d) Parameter δ.

FIGURE 6 – Confidence intervals of α-stable parameters.

of rate success is approximately 97 % for the α-stable, 50 % for the Weibull distribution and 10 % for the $\mathcal{K}$ distribution. The Weibull and $\mathcal{K}$ distributions are not adequate for modeling the probability density function of sea surface RCS. Indeed, the boxplots of p-value and KSSTAT (Figure 5) show there are fewer errors with the α-stable law. The estimation of the probability density function shows also that the Weibull and $\mathcal{K}$ distributions are not suitable to fit the data (Figure 4). The α-stable distribution is characterized by an infinite variance which indicates it does not directly translate to a physical model. This property has an impact on a random process of a scattering coefficient. Indeed, extreme values can be observed in Figure 7. The extreme values are dependent of the deterministic sea surface. We continue the study by calculating a confidence interval for the parameters of α-stable distribution.

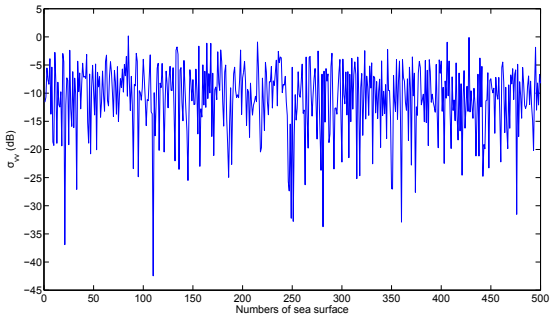

FIGURE 7 – Example of 500 sea surface RCS.

4.2 Confidence intervals

A confidence interval gives an estimated range of α-stable parameter values : the lower bound corresponds to the first quartile and the upper bound is the third quartile. We plot also the probability value of each parameter. The Figure 6(b) shows the parameter β is closed to -1. Indeed, the probability of the parameter $\beta = -1$ is high (Figure 8) and could be fixed to -1. It is difficult to extract a law for the parameter α (Figure 6(a)) and the probability of $\alpha = 2$ is high. It is the same analysis for the parameter γ (Figure 6(c)). However, the probability value of γ could be modeled by a Gaussian distribution (Figure 8). In Figure 8, we can observe three modes : the mode around 30 corresponds to the diagonal in Figure 6(d), the mode around 20 corresponds to the value closed to the diagonal and the mode around -25 corresponds to the other values. However, it is difficult to

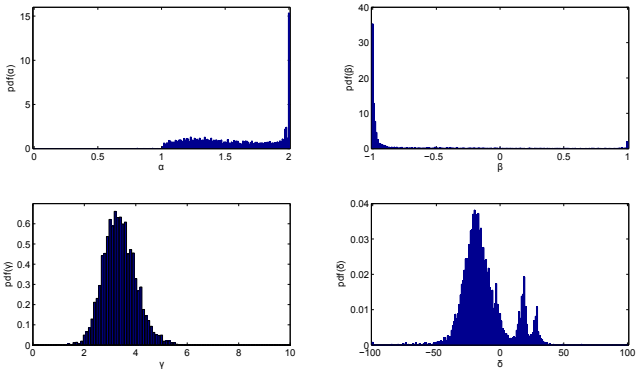

FIGURE 8 – Probability of parameter.

extract information from confidence intervals : we choose to work with the probability density function of estimated parameters. The next section analyses the influence of polarizations, wind direction and wind speed on probability density functions of α-stable parameters.

4.3 Influence of parameters

In this section, 24 configurations are analyzed by varying polarizations (HH,VV, VH and HV), wind speed (3m/s and 5m/s) and wind direction ($0°$, $25°$ and $60°$).

4.3.1 Parameters α, β and γ

The probability density functions of parameters α, β and γ have been superposed (Figure 9). The probability density functions are independent of polarizations, wind speed and direction of speed. Consequently, these parameters can not be use to discriminate the different configurations.

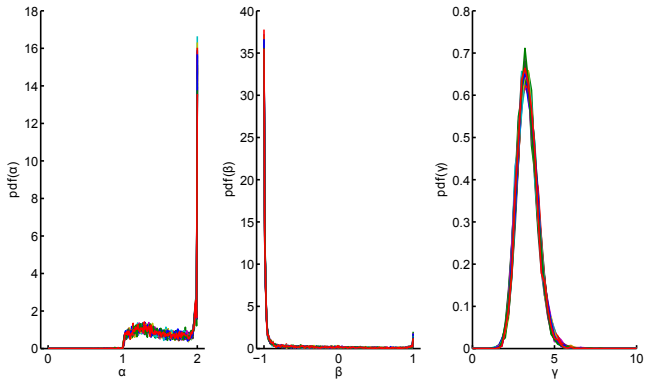

FIGURE 9 – Represantation of probability density functions for the parameters α, β and γ.

4.3.2 Parameter δ

We observe firstly the influence of the polarization on the probability density function of δ. The configuration used is defined by : wind speed v=3 m/s and wind direction $\psi = 0°$. The co-polarizations (HH and VV) and the cross-polarizations (VH and HV) give similar results. The cross-polarizations HV and VH can be discriminated. Indeed, the modes are shifted. The probability density functions obtained for cross-polarizations have three modes against two modes for co-polarizations.

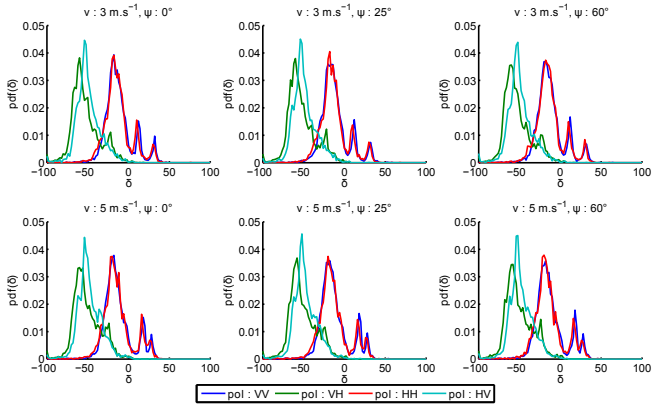

FIGURE 10 – Influence of polarization on probability density function of parameter δ.

To analyze the influence of wind speed, polarization and wind direction are fixed. We consider firstly the co-polarization VV with wind direction $\psi = 0°$. We observe a mode at -18 in common, which represents the most probable value. Two modes smaller for the wind speed 3 m/s are visible at the values 12 and 32. These values are different for the wind speed 5 m/s and are equal to 18 and 38.

The smallest mode corresponds to the case $\theta_i = \theta_s$. The same conclusions can be made for wind directions $\psi = 25°$ and $\psi = 60°$. For the polarization VV, the values of modes are equals to 30 and 10 for the wind speed 3 m/s and 16 and 26 for the wind speed 5 m/s.

For the cross-polarizations, the analysis is different. Indeed, we observe only two modes. The representation of the probability density function could be fit with a Gaussian. However, a small pick is visible. For the polarization HV, the probability density function of parameter δ for the wind speed 3 m/s is less than to the wind speed 5 m/s for the values belonging to [-40,-20]. It is more difficult to make the same observation for the polarization VH.

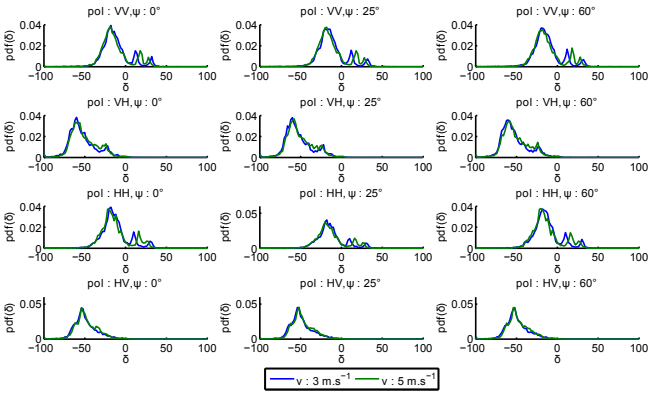

FIGURE 11 – Influence of wind speed on probability density function of parameter δ.

To observe the influence of wind direction on the probability density function of position parameter δ, the polarization and the wind speed are fixed. The configuration used is defined by the polarization VV and wind speed v=5 m/s. We observe three modes with values -18, 18 and 28 for any wind direction. Curves are superimposed irrespective of wind direction. The same analysis can be made for the wind speed v=5 m/s but the modes are shifted. The representation of probability density function is independent of wind direction.

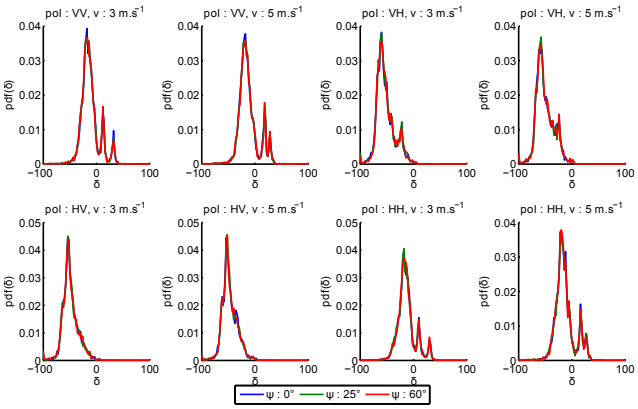

FIGURE 12 – Influence of direction of wind on probability density function of parameter δ.

4.4 Statistical models for probability of detection

Denote P_A the sea surface RCS probability density function and P_T the target RCS probability density function. We assume that P_A and P_T are characterized by heavy-tails and the hypothesis "sea surface RCS and target RCS can be modeled by α-stable distribution" are verified by the Kolmogorov-Smirnov test. For a fixed threshold Z, the probabilities of detection (P_D) and false alarm (P_{FA}) can be expressed by :

$$P_D = \int_Z^{+\infty} P_T(z)dz, P_{FA} = \int_Z^{+\infty} P_A(z)dz, \quad (10)$$

The values of integrals are defined by the cumulative density function of estimated model. We also estimate the sea surface RCS with a $\mathcal{K}$ distribution. We plot the probability of detection versus probability of false alarm (also known a Receiver Operation Characteristic (ROC) curve) for the two hypothesis (Figure 13). The detection performance with the

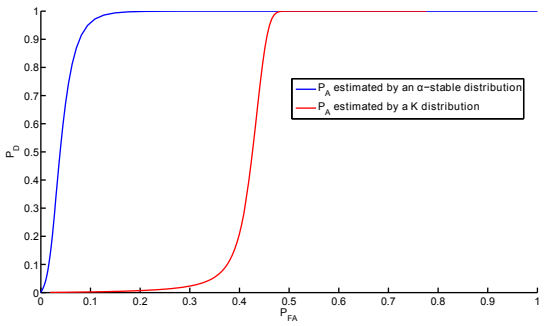

FIGURE 13 – Two ROC curves plotted on linear axes.

α-stable distribution is significantly better than that associated with the $\mathcal{K}$ distribution. Consequently, the impact of distribution errors on detection performance can be increase with an inappropriate model of estimation.

5 Conclusion

In this paper, we propose a comparative statistical study of the sea surface. The sea surface RCS probability density function is characterized by heavy-tails and asymmetry. Three models of estimation are compared with a Kolmogorov-Smirnov test : Weibull, $\mathcal{K}$, and α-stable distributions. The Kolmogorov-Smirnov test shows that the α-stable distribution gives the best fit compared to the Weibull distribution and the $\mathcal{K}$-distribution. The performance of detection with the α-stable is better than associated with the $\mathcal{K}$ distribution, assuming data are modeled by an α-stable distribution.

Références

[1] M. Abramowitz and I.A. Stegun. *Handbook of mathematical functions with formulas, graphs, and mathematical tables*, volume 55. Dover publications, 1964.

[2] A. Achim, P. Tsakalides, and A. Bezerianos. Sar image denoising via bayesian wavelet shrinkage based on heavy-tailed modeling. *IEEE Transactions on Geoscience and Remote Sensing*, 41(8) :1773–1784, 2003.

[3] A. Banerjee, P. Burlina, and R. Chellappa. Adaptive target detection in foliage-penetrating sar images using alpha-stable models. *IEEE Transactions on Image Processing*, 8(12) :1823–1831, 1999.

[4] A. Baussard, M. Rochdi, and A. Khenchaf. Po/mec-based scattering model for complex objects on a sea surface. *Progress In Electromagnetics Research*, 111 :229–251, 2011.

[5] C. Cox and W. Munk. Statistics of the sea surface derived from sun glitter. *Journal of Marine Research*, 13(2) :198–227, 1954.

[6] C. Cox and W. Munk. Slopes of the sea surface deduced from photographs of sun glitter. *Bulletin of the Scripps Institution of Oceanography*, 6(9) :401–488, 1956.

[7] M.L.X. Dos Santos and N.R. Rabelo. On the ludwig integration algorithm for triangular subregions. *Proceedings of the IEEE*, 74(10) :1455–1456, 1986.

[8] T. Elfouhaily, B. Chapron, K. Katsaros, and D. Vandemark. A unified directional spectrum for long and short wind-driven waves. *Journal of Geophysical Research*, 102(C7) :15781–15, 1997.

[9] F.A. Fay, J. Clarke, and R.S. Peters. Weibull distribution applied to sea clutter. pages 101–104, 1977.

[10] E. Jakeman and P. Pusey. A model for non-rayleigh sea echo. *IEEE Transactions on Antennas and Propagation*, 24(6) :806–814, 1976.

[11] L. Klein and C. Swift. An improved model for the dielectric constant of sea water at microwave frequencies. *IEEE Transactions on Antennas and Propagation*, 25(1) :104–111, 1977.

[12] P. Lévy. Théorie des erreurs : La loi de gauss et les lois exceptionelles. *Bulletin de la Société Mathématique de France*, 52 :49–85, 1924.

[13] R.D. Pierce. Rcs characterization using the alpha-stable distribution. In *Proccedings of Radar Conference, 1996*, pages 154–159, 1996.

[14] D.C. Schleher. Radar detection in weibull clutter. *IEEE Transactions on Aerospace and Electronic Systems*, (6) :736–743, 1976.

[15] A.G. Voronovich. *Wave scattering from rough surfaces*. Springer Berlin, 1999.

[16] K.D. Ward, C.J. Baker, and S. Watts. Maritime surveillance radar. i. radar scattering from the ocean surface. In *IEE Proceedings F Radar and Signal Processing*, volume 137, pages 51–62. IET, 1990.

[17] K.D. Ward, S. Watts, and R.J.A. Tough. *Sea clutter : scattering, the K-distribution and radar performance*, volume 20. Institution for Engineering and Technology, 2006.

[18] W. Weibull. A statistical distribution function of wide applicability. *Journal of applied mechanics*, 1951.

[19] V.M. Zolotarev. *One-dimensional stable distributions*, volume 65. American Mathematical Society, 1986.